

tical. In Ref. 1, the following description of the steady flowfield is presented for the isolated airfoil. The flow is completely subsonic at Mach numbers below  $M_\infty=0.775$ . A weak shock wave exists around midchord at  $M_\infty=0.8$ ; the shock is at the three-quarter chord point at  $M_\infty=0.85$ . At  $M_\infty=0.9$ , the fish-tail shock pattern appears.

Thus, it can be seen that some of the flow characteristics are similar in the cascade and isolated airfoil steady results. The shock is at the midchord location when  $M_\infty=0.68$  for the cascade and  $M_\infty=0.8$  for the isolated airfoil. Taking into account this difference, it can be seen that the present results are almost identical to the isolated airfoil results. However, note that the shock reaches the trailing edge at  $M_\infty=0.7$  in the cascade whereas for the isolated airfoil the corresponding value is  $M_\infty=0.9$ . This shows that the shock location changes more rapidly in the cascade as the Mach number is changed from 0.68 to 0.7. Furthermore, the choking observed in the present cascade flow has no corresponding feature in isolated airfoil flow. Thus, although many similarities can be observed between the cascade results and the isolated airfoil results, distinct differences remain.

### Concluding Remarks

Flutter calculations have been performed for an unstaggered NACA 64A010 cascade using the frequency-domain method. A comparison of the present results with isolated airfoil theory based on a transonic small-disturbance analysis shows that the flutter results are similar. The significant difference is a shift in the flutter velocity variation along the Mach number axis. It is concluded that the significant phenomena that lead to the distinct variations in flutter speed are present in both the isolated airfoil and cascade flows. However, a distinct difference between the two flows is the choking of the flow in the cascade. Because of this difference, a complete quantitative correlation of the two results is not expected.

### References

- <sup>1</sup>Isogai, K., "Numerical Study of Transonic Flutter of a Two-Dimensional Airfoil," National Aerospace Lab., Tokyo, Japan, NAL-TR-617T, July 1980.
- <sup>2</sup>Isogai, K., "On the Transonic-Dip Mechanism of Flutter of a Sweptback Wing," *AIAA Journal*, Vol. 17, No. 7, 1979, pp. 793-795.
- <sup>3</sup>Kao, Y. F., "A Two-Dimensional Unsteady Analysis for Transonic and Supersonic Cascade Flows," Ph.D. Thesis, School of Aeronautics and Astronautics, Purdue Univ., West Lafayette, IN, May 1989.
- <sup>4</sup>Bakhle, M. A., Reddy, T. S. R., and Keith, T. G., Jr., "Time-Domain Flutter Analysis of Cascades Using a Full-Potential Solver," *AIAA Journal*, Vol. 30, No. 1, 1992, pp. 163-170.
- <sup>5</sup>Bakhle, M. A., Mahajan, A. J., Keith, T. G., Jr., and Stefkó, G. L., "Cascade Flutter Analysis with Transient Response Aerodynamics," *Computers and Structures*, Vol. 41, No. 5, 1991, pp. 1073-1085.
- <sup>6</sup>Verdon, J. M., and Caspar, J. R., "A Linear Aerodynamic Analysis for Unsteady Transonic Cascades," NASA CR-3833, Sept. 1984.
- <sup>7</sup>Bakhle, M. A., Reddy, T. S. R., and Keith, T. G., Jr., "An Investigation of Cascade Flutter Using a Two-Dimensional Full-Potential Solver," AIAA Paper 92-2119, April 1992.

## Supersonic Panel Flutter Analysis of Shallow Shells

Maher N. Bismarck-Nasr\*

Instituto Tecnológico de Aeronáutica,  
São José dos Campos, SP, 12228-900, Brazil

### I. Introduction

**F**LUTTER characteristics determination of shallow shells is of prime importance in supersonic aircraft and launch vehicle designs. The first analytical research on supersonic

flutter of thin cylindrically curved panels was made by Voss,<sup>1</sup> using Reissner's shallow shell equations,<sup>2</sup> quasistatic aerodynamic theory, and the Galerkin method for the solution of freely supported ends boundary conditions. Nonlinear flutter analysis of two-dimensional<sup>3</sup> and three-dimensional<sup>4</sup> curved panels were performed by Dowell using a quasistatic aerodynamic theory. Dowell's investigations showed that the in-plane edge restraints had a great influence on the flutter boundaries, and this phenomenon was attributed to the frequency spectrum of the shells analyzed. Since Olson<sup>5</sup> introduced the aerodynamic matrix concept, many authors exploited the application of the finite element method in the field of supersonic panel flutter.<sup>6</sup> Reissner's two field variables principle<sup>7</sup> with transverse displacement and Airy stress functions taken as field variables represents an efficient alternative for the treatment of shallow shell problems. In spite of the simplifications it introduces, Reissner's principle is scarcely used in finite element formulation. The main reason is attributed to the difficulties encountered when applying the boundary conditions on Airy stress function.<sup>8-9</sup> In Ref. 10, starting from Reissner's variational equation for the free vibration of cylindrically curved panels, the Euler-Lagrange equations and the boundary conditions of the problem were deduced. It was shown that the boundary conditions on Airy stress functions are as simple and direct to apply as on the transverse displacements. The purpose of the present work is to present a finite element analysis of the supersonic flutter of cylindrically curved panels based on Reissner's two field variational principle.

### II. Problem Formulation

The variational equation of thin cylindrically curved shallow shells,<sup>7</sup> Fig. 1., reads

$$\delta(\Pi^*) = \delta \left\{ \frac{1}{2} \int_A \rho h w_{,t}^2 dA - \frac{D}{2} \int_A [w_{,xx}^2 + w_{,yy}^2 + 2\nu w_{,xx} w_{,yy} + 2(1-\nu)w_{,xy}^2] dA + \frac{1}{2Eh} \int_A [F_{,xx}^2 + F_{,yy}^2 - 2\nu F_{,xx} F_{,yy} + 2(1+\nu)F_{,xy}^2] dA - \int_A \frac{w}{R} F_{,xx} dA + \int_A w \Delta p dA \right\} = 0 \quad (1)$$

In Eq. (1),  $\rho$  is the material mass density per unit of area,  $h$  is the shell thickness,  $D = Eh^3/12(1-\nu^2)$  is the shell flexural rigidity,  $\nu$  is Poisson's ratio,  $E$  is Young's modulus, and  $\Delta p$  is the aerodynamic pressure difference. Using the quasistatic aerodynamic theory, the relationship between  $\Delta p$  and  $w$  can be written as

$$\Delta p = -\frac{2Q}{\sqrt{M^2-1}} \frac{\partial w}{\partial x} \quad (2)$$

where  $Q = \rho V^2/2$  is the dynamic pressure,  $M$  and  $V$  are the freestream Mach number and velocity, respectively. Performing the variational operation, grouping terms, and applying Green's theorem, the Euler-Lagrange equations of the problem are obtained and read

$$D \nabla^4 w + \frac{1}{R} F_{,xx} + \rho h w_{,tt} - \frac{2Q}{\sqrt{M^2-1}} w_{,x} = 0 \quad (3)$$

$$\nabla^4 F - \frac{Eh}{R} w_{,xx} = 0 \quad (4)$$

and the classical boundary conditions on an edge  $\mu = \text{constant}$ , where  $\mu$  stands for  $x$  or  $y$ , and  $\eta$  normal to  $\mu$  direction are given by

$$\text{Clamped edge } w = w_{,\mu} = 0 \text{ and at a corner } F_{,\mu\eta} = 0 \quad (5a)$$

$$\text{Free edge } F = F_{,\mu} = 0 \text{ and at a corner } M_{,\mu\eta} = 0$$

$$(\text{i.e., } w_{,\mu\eta} = 0) \quad (5b)$$

Received July 28, 1992; revision received Dec. 17, 1992; accepted for publication Dec. 17, 1992. Copyright © 1992 by the American Institute of Aeronautics and Astronautics, Inc. All rights reserved.

\*Professor, Division of Aeronautical Engineering. Member AIAA.

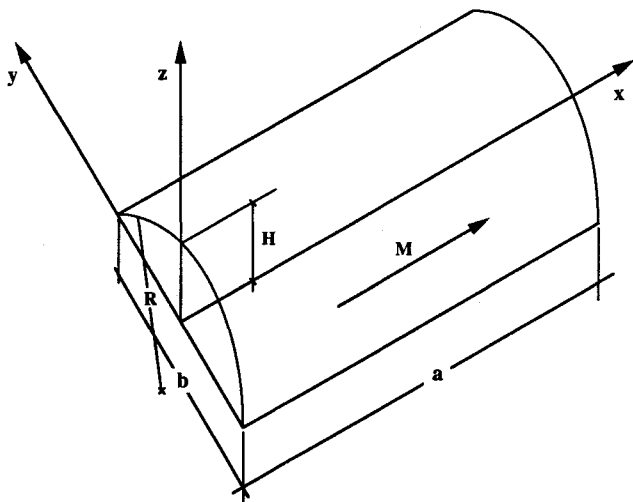


Fig. 1 Shell geometry and notations.

Simply supported edge  $w = 0$  and at a corner  $F_{,\mu\eta} = 0$  (5c)

Freely supported edge  $w = F = 0$  (5d)

A finite element solution for the problem at hand can be performed using rectangular elements preserving  $C^1$  continuity based on the functional given in Eq. (1). Thus, we can write

$$z(x, y) = \sum_{i=1}^2 \sum_{j=1}^2 [H_{0i}(x)H_{0j}(y)z_{ij} + H_{1i}(x)H_{0j}(y)z_{,xij} + H_{0i}(x)H_{1j}(y)z_{,yij} + H_{1i}(x)H_{1j}(y)z_{,xyij}] \quad (6)$$

where  $z$  stands for  $w$  or  $F$  and  $H_{mn}$  are first-order Hermitian polynomials; other notations are as given in Ref. 11. Using the standard finite element technique, we obtain for each element a set of two equations cast in the following form:

$$[k_{ww}]\{w\} + [k_{wF}]\{F\} + [m]\{\ddot{w}\} + \lambda[a]\{w\} = \{0\} \quad (7a)$$

$$[k_{Fw}]\{w\} + [k_{FF}]\{F\} = \{0\} \quad (7b)$$

where  $\lambda = 2Q/\sqrt{M^2 - 1}$  is the dynamic pressure parameter. The matrices in Eq. (7) can be calculated as given in Refs. 10 and 11. Using the finite element standard assembly technique and applying the appropriate boundary conditions, the equations read

$$[K_{ww}]\{w\} + [K_{wF}]\{F\} + [M]\{\ddot{w}\} + \lambda[A]\{w\} = \{0\} \quad (8a)$$

$$[K_{Fw}]\{w\} + [K_{FF}]\{F\} = \{0\} \quad (8b)$$

The degrees of freedom  $\{F\}$  can be eliminated using the compatibility Eq. (8b), reducing the aeroelastic problem to

$$[K_{eq}]\{w\} + [M]\{\ddot{w}\} + \lambda[A]\{w\} = \{0\} \quad (9)$$

where,  $[K_{eq}] = [K_{ww}] - [K_{wF}][K_{FF}]^{-1}[K_{Fw}]$ . An examination of Eq. (9) reveals that the computational effort required for the solution of the aeroelastic problem is equivalent to that of a flat plate problem when the present formulation is used. The inplane boundary conditions are applied on  $F$ ,  $F_{,x}$ ,  $F_{,y}$ , and  $F_{,xy}$ , and are all nodal degrees of freedom.

### III. Numerical Results

Results of some computations using the present formulation are reported in this section. For simplicity, only square cylindrically curved panels have been considered, and the results are presented in terms of the critical dynamic pressure parameter  $\lambda_{cr} = \lambda a^3/D$  as a function of the maximum shell rise  $H/h$ . The first series of calculations was performed for freely sup-

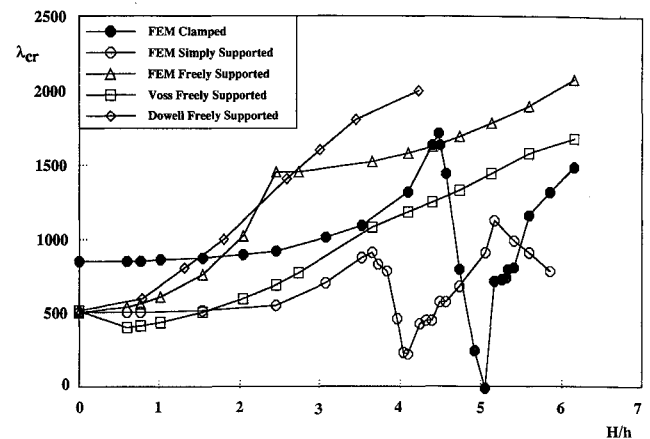


Fig. 2 Flutter dynamic pressure vs shell rise.

ported end conditions to compare the results of the natural frequencies calculations with the exact analytical solution using Reissner's equation.<sup>2</sup> It is anticipated that for the curved panels with the increase of the curvature, higher modes will coalesce first to produce the critical flutter condition. Therefore, the finite element model used must maintain good precision for a wide range of the frequency spectrum. Using a mesh of  $4 \times 4$  elements, the calculations showed that the error in the natural frequencies ranged from 1% for the first to 4% for the 15th mode. This precision was considered sufficient enough to proceed for the aeroelastic calculations using a mesh of  $4 \times 4$ . The results of  $\lambda_{cr}$  are shown in Fig. 2 and are compared with the previous solutions of Voss<sup>1</sup> and Dowell.<sup>4</sup> Voss's solution is a two-term Galerkin approximation and shows the same trend as the present formulation. Dowell's solution is a six-chordwise-modes Galerkin approximation with a half-sine wave in the cross-stream direction and practically coincides with the present solution for the parts of the curve where  $n = 1$  are the critical modes. Simply supported and clamped edges panels are then analyzed, and the results are shown in Fig. 2. From these results it can be observed that for a curvature effect up to  $H/h = 2$ , the critical flutter modes are the first modes and  $\lambda_{cr}$  is practically the same as for a flat panel. With the increase of the curvature, higher modes coalesce first, and the coalescence is characterized by the decrease or increase of the critical dynamic pressure parameter. In the region of flat plate behavior, the curvature effect is stabilizing in the sense that  $\lambda_{cr}$  increases with the increase of the curvature. With further increase of the curvature, the panel passes through a transition region characterized from a flat plate to a deep shell behavior. This region is characterized by the dips, knees, and cups observed in  $\lambda_{cr}$  vs curvature, and is explained by the coalescence of successive higher modes. After this transition region, the panel behaves as a deep shell, and  $\lambda_{cr}$  is for an elevated number of waves in the cross-stream direction and the first spanwise modes. For clarity of the exposition, no damping effect, whether of structural or of aerodynamic nature has been incorporated. If a constant viscous-type structural damping and/or the aerodynamic damping term of the linear potential flow theory are used in the analysis, it can be shown that their effect is always stabilizing.<sup>6</sup> The effect of such damping is small in the flat plate behavior and deep shell regions. In the transition region, such dampings have a greater influence on the stability of the panel and remove the sharp minima or dips, which are due to coalescence of modes with nearly identical frequencies and small aerodynamic coupling.<sup>6</sup>

### IV. Concluding Remarks

Finite element solutions of the supersonic flutter of cylindrically curved panels have been presented. Reissner's two field variables variational principle has been used to formulate a  $C^1$  continuity element that satisfies the requirements of the finite

element method. Previous investigations have demonstrated that the inplane edge restraints have a great influence on the flutter boundaries. The present finite element formulation permits a direct and exact application of the inplane end conditions for all classical boundary conditions.

### Acknowledgment

Grant 300954/91-3 (NV) of Conselho Nacional de Desenvolvimento Científico e Tecnológico-Brasil (CNPq) conceded to the author during the preparation of this work is gratefully acknowledged.

### References

- <sup>1</sup>Voss, H. M., "The Effect of an External Supersonic Flow on the Vibration Characteristics of Thin Cylindrical Shells," *Journal of Aero/Space Sciences*, Vol. 28, No. 12, 1961, pp. 945-956.
- <sup>2</sup>Reissner, E., "On Transverse Vibrations of Thin, Shallow Elastic Shells," *Quarterly of Applied Mathematics*, Vol. 13, No. 2, 1955, pp. 169-176.
- <sup>3</sup>Dowell, E. H., "Nonlinear Flutter of Curved Plates," *AIAA Journal*, Vol. 7, No. 3, 1969, pp. 424-431.
- <sup>4</sup>Dowell, E. H., "Nonlinear Flutter of Curved Plates II," *AIAA Journal*, Vol. 8, No. 2, 1970, pp. 259-261.
- <sup>5</sup>Olson, M. D., "Finite Elements Applied to Panel Flutter," *AIAA Journal*, Vol. 5, No. 12, 1967, pp. 2267-2270.
- <sup>6</sup>Bismarck-Nasr, M. N., "Analysis of Aeroelasticity of Plates and Shells," *Applied Mechanics Reviews*, Vol. 45, No. 12, Pt. 1, 1992, pp. 461-482.
- <sup>7</sup>Reissner, E., "On a Variational Theorem for Finite Elastic Deformation," *Journal of Mathematics and Physics*, Vol. 32, No. 2-3, 1953-1954, pp. 129-135.
- <sup>8</sup>Gass, N., and Tabarrok, B., "Large Deformation Analysis of Plates and Cylindrical Shells by a Mixed Finite Element Method," *International Journal for Numerical Methods in Engineering*, Vol. 10, No. 4, 1976, pp. 731-746.
- <sup>9</sup>Gallagher, R. H., Heinrich, J. C., and Sarigul, N., "Complementary Energy Revisited," *Hybrid and Mixed Finite Element Methods*, edited by S. N. Atluri, R. H. Gallagher, and O. C. Zienkiewicz, Wiley, New York, 1983.
- <sup>10</sup>Bismarck-Nasr, M. N., "On Vibration of Thin Cylindrically Curved Panels," *Proc. III PACAM, Third Pan American Congress of Applied Mechanics*, São Paulo, Brazil, Jan, 4-8, 1993, pp. 696-699.
- <sup>11</sup>Bismarck-Nasr, M. N., "On the Sixteen Degree of Freedom Rectangular Plate Element," *International Journal of Computers and Structures*, Vol. 40, No. 4, 1991, pp. 1059-1060.

## Stability Criteria of Structural Control with Systems Noncolocated Velocity Feedback

Shih-Ming Yang\*

National Cheng Kung University, Taiwan,  
Republic of China

### Introduction

FEEDBACK control with a colocated sensor and actuator has been considered having stability robustness. A sensor and actuator pair at the same location is often referred to as colocated, and any dislocation of the pair is considered a noncolocated configuration. Such a definition of colocated and noncolocated feedback is the only one meaningful in structural control implementation and experimentation. Previous work identifying the same definition of noncolocated feedback includes that of Schafer and Holzach<sup>1</sup> and Parks and Pak.<sup>2</sup> Balas<sup>3</sup> was among the first to con-

sider velocity feedback with a colocated sensor and actuator. In the absence of actuator dynamics, this technique is unconditionally stable. However, having the option to use noncolocated feedback is often desirable because of design flexibility. In addition, noncolocated feedback may often be required due to physical limitation and/or hardware constraint. In the study of control/structure synthesis, Thomas and Schmit<sup>4</sup> considered noncolocated velocity and displacement feedback to a cantilever beam system. Because of the sensor and actuator placement, they were unable to achieve stability robustness. Cannon and Rosenthal<sup>5</sup> applied noncolocated feedback to a flexible structure control experiment and concluded that effective noncolocated feedback is one of the major challenges to large space structure application.

In flexible structure vibration control, the structure system is normally discretized either by finite element method or by normal mode analysis. The governing equation is hence written in the form of second-order differential equations with sparse or diagonal inertia, damping, and stiffness coefficient matrices. Prediction of stability robustness by calculating the closed-loop system spectrum for a given set of system parameters, including structural modal properties, sensor/actuator placement, and control law, is straightforward but tedious for a reasonably large number of parameters. One may argue that by keeping the mass, damping, and stiffness matrices of the closed-loop system positive definite, then the asymptotic stability is guaranteed; however, such a criterion is no longer valid in the case of noncolocated feedback because these coefficient matrices can be asymmetric. Thus, the need of design guidelines for both the control law and sensor/actuator placement that guarantee an asymptotically stable system is evident. This Note investigates the stability of second-order structural control systems with noncolocated velocity feedback. Robust stability criteria are developed for structural control in the absence of sensor and actuator dynamics. Conditions are derived such that the closed-loop system is asymptotically stable with infinite gain margin. These conditions are stated in terms of the structure system parameters such as inertia, damping, and stiffness matrices; sensor/actuator placement; and feedback control gain matrix.

### Velocity Feedback

In the analysis and design of structural control, the governing equation of motion of a discretized system is often written as

$$\ddot{x} + C\dot{x} + \Lambda x = Bu \quad (1)$$

where  $x$  is an  $n \times 1$  generalized coordinate vector.  $C$  is a symmetric, positive definite damping matrix, denote  $C > 0$ .  $\Lambda$  is a symmetric stiffness matrix,  $\Lambda > 0$  for most structure systems; however, it can also be a negative definite,  $\Lambda < 0$ , in stable gyroscopic systems or statically unstable systems. Note that the identity inertia matrix indicates that normal modes discretization is applied in the formulation. All coefficient matrices are of dimension  $n \times n$ , the actuator influence matrix  $B$  is of  $n \times m$ , and the control force  $u$  is of  $m \times 1$ .

Although the requirement of direct velocity measurement may be restrictive in hardware implementation, colocated velocity feedback is the most widely discussed method in the structural control studies for its positive damping argumentation. Such control law makes the closed-loop system asymptotically stable with infinite gain margin. The system dynamics can be described by  $n$  modes with no residual modes, and the feedback controller is

$$u = -K_v B_v^T \dot{x} \quad (2)$$

where  $K_v$  is the velocity feedback control gain matrices, and  $B_v$  is the measurement sensor influence matrix. Substituting Eq. (2) into Eq. (1), the feedback control system becomes

$$\ddot{x} + (C + BK_v B_v^T) \dot{x} + \Lambda x = 0 \quad (3)$$

$$\ddot{x} + (D + G) \dot{x} + \Lambda x = 0 \quad (4)$$

where  $D$  and  $G$  are termed generalized damping and gyroscopic matrices, respectively.

$$D = C + 1/2 (BK_v B_v^T + B_v K_v^T B^T)$$

$$G = 1/2 (BK_v B_v^T + B_v K_v^T B^T)$$

Received Aug. 4, 1992; revision received Dec. 17, 1992; accepted for publication Dec. 17, 1992. Copyright © 1993 by the American Institute of Aeronautics and Astronautics, Inc. All rights reserved.

\*Associate Professor, Institute of Aeronautics and Astronautics. Associate Member AIAA.